Potential Gallium-68 Tracers for Imaging the Heart with PET: Evaluation of Four Gallium Complexes with Functionalized Tripodal *Tris*(Salicylaldimine) Ligands

Mark A. Green, Carla J. Mathias, William L. Neumann, Phillip E. Fanwick, Michael Janik and Edward A. Deutsch

Departments of Medicinal Chemistry and Chemistry, Purdue University, West Lafayette, Indiana and Mallinckrodt Medical, Inc., St. Louis, Missouri

Gallium-67 and ^{68}Ga complexes have been synthesized with tripodal hexadentate salicylaldimine ligands derived from 1,1,1-*tris*(salicylaldiminomethyl)ethane, sal$_3$tame. The four ligands evaluated contained alkoxy substituents (*n*-BuO-, *iso*-BuO-, *sec*-BuO-, and *n*-PrO-) on the terminal ethane carbon of the ligand backbone. In the case of the *n*-PrO-derivative, the *tris*(salicylaldimine) ligand was additionally substituted with methoxy groups in the 5-position of the aromatic rings. The ^{67}Ga and ^{68}Ga-complexes of these ligands were prepared by ligand exchange from ^{67}Ga- or ^{68}Ga-acetylacetonate in ethanol. The nonradioactive Ga[(sal)$_3$tame-O-*iso*-Bu] complex was similarly prepared and shown by x-ray crystallography to exhibit the expected pseudo-octahedral $N_3O_3^{3-}$ coordination sphere about the Ga^{3+} center. These Ga-radiotracers are highly lipophilic, as demonstrated by their octanol/water partition coefficients. Log *P* values of 3.1, 3.1, 2.6, and 2.5 were found for the [(sal)$_3$tame-O-*iso*-Bu], [(sal)$_3$tame-O-*n*-Bu], [(sal)$_3$tame-O-*sec*-Bu], and [(5-MeOsal)$_3$tame-O-*n*-Pr] complexes, respectively. Following intravenous injection into rats, these complexes are rapidly cleared from the blood and exhibit significant myocardial uptake. At 1 min postinjection, 2.4%, 2.0%, 2.1% and 1.1% of the injected dose was found in the heart for the *iso*-BuO, *n*-BuO, *sec*-BuO, and *n*-PrO complexes, respectively, dropping to 1.0%, 0.8%, 0.8%, and 0.7% at 5 min. The corresponding heart-to-blood ratios are quite high: 17 ± 3, 14 ± 2, 12 ± 2 and 3.5 ± 0.4 at 1 min and 14 ± 4, 10 ± 1, 10 ± 1 and 3.2 ± 0.1 at 5 min postinjection. High quality myocardial images were obtained with PET in a normal dog using data collected from 2 to 10 min following intravenous injection of ^{68}Ga[(sal)$_3$tame-O-*iso*-Bu].

J Nucl Med 1993; 34:228–233

The widespread use of positron emission tomography (PET) in diagnostic medicine could be facilitated by increased availability of positron-emitting radiopharmaceuticals labeled with generator-produced nuclides (*1*). The ^{68}Ge/^{68}Ga parent/daughter generator system is especially attractive as a PET radionuclide source due to the long half-life of the ^{68}Ge parent (271 days) combined with the reasonably short half-life of the ^{68}Ga daughter (68 min). Unfortunately, despite the attractive nuclear properties of this parent/daughter pair, only limited success has been realized in attempts to deliver clinically useful PET radiopharmaceuticals labeled with ^{68}Ga (*1,2*).

The clinical importance of myocardial perfusion imaging with PET has led to a number of attempts to prepare ^{68}Ga-labeled blood flow tracers (*1–7*). Uncharged, lipophilic Ga(III) complexes of 1,1,1-*tris*-(salicylaldiminomethyl)ethane [(sal)$_3$tame] and 1,1,1-*tris*-(alkoxysalicylaldiminomethyl)ethane [(ROsal)$_3$tame] have been investigated as ^{68}Ga heart imaging agents with limited success (*3,4*). Following intravenous injection, these complexes resist ligand exchange with transferrin, an abundant plasma protein (2–4 g/liter) with two high-affinity binding sites for the Ga^{3+} ion ($log\ K_1^* = 20.3$; $log\ K_2^* = 19.3$) (*8*). Gallium-68-[(5-MeOsal)$_3$tame] allowed qualitative PET imaging of myocardial perfusion in the dog (*3*); however, the properties of this tracer do not make it an adequate substitute for cyclotron-produced PET myocardial blood flow tracers. Although ^{68}Ga uptake was found to increase with the rate of myocardial perfusion, it was shown using isolated perfused hearts that both the extraction fraction and the rate of tracer clearance from myocardium are flow-dependent (*3*). It also proved necessary to correct ^{68}Ga[(5-MeOsal)$_3$tame] myocardial images for radioactivity remaining in the ventricular blood pool, due to inadequate contrast between heart and blood at short times postinjection. More recently, a cationic ^{68}Ga-radiopharmaceutical, Ga(BAT-TECH)$^{1+}$ has been described and evaluated as a PET agent for imaging the heart (*6,7*), improving somewhat on ^{68}Ga[(5-MeOsal)$_3$tame] with higher heart uptake and lower blood levels of tracer (*1,3,7*).

We report here evaluation of four new tripodal hexadentate *tris*(salicylaldimine) ligands and assessment of

Received May 26, 1992; revision accepted Sept. 2, 1992.

For correspondence or reprints contact: Mark A. Green, PhD, Department of Medicinal Chemistry, Pharmacy Building, Purdue University, West Lafayette, IN 47907.

their potential for providing novel ^{68}Ga-radiopharmaceuticals. These four ligands contain alkoxy-substituents on the ethane backbone of the triamine framework (Fig. 1) that serve to make the corresponding gallium radiotracers substantially more lipophilic than the derivatives previously studied and result in radiopharmaceuticals that can be used to obtain high-quality PET images of the heart without blood-pool subtraction.

MATERIALS AND METHODS

The four *tris*(salicylaldimine) ligands (Fig. 1) were obtained by condensation of salicylaldehyde or 5-methoxysalicylaldehyde with the appropriate derivative of 1,1,1-*tris*(aminomethyl)ethane (*3,9,10*). Gallium-67-chloride in HCl solution was obtained from Mallinckrodt Medical, Inc., St. Louis, while ^{68}Ga-chloride was obtained in 1 N HCl from an ionic ^{68}Ge/^{68}Ga tin dioxide generator (*11*) purchased from DuPont/New England Nuclear, N. Billerica, MA.

The complexes of these four *tris*(salicylaldimine) ligands with nonradioactive gallium were each prepared by reaction of *tris*(2,4-pentanedionato)gallium(III), Ga(acac)$_3$, with a 5% excess of the *tris*(salicylaldimine) ligand in hot ethanol following the general procedure described previously (*3,12*). All showed the expected parent ion peaks in their electron impact mass spectra: m/e = 567 for the $[C_{30}H_{32}N_3O_4{}^{69}Ga]^+$ ions of the Ga[(sal)$_3$tame-O-*n*-Bu] , Ga[(sal)$_3$tame-O-*iso*-Bu] and Ga[(sal)$_3$tame-O-*sec*-Bu] isomers and m/e = 643 for the $[C_{32}H_{36}N_3O_7{}^{69}Ga]^+$ ion of Ga[(5-MeOsal)$_3$tame-O-*n*-Pr]. Analysis for Ga[(sal)$_3$tame-O-*n*-Bu] (m.p. 294°C)-Calculated for $C_{30}H_{32}N_3O_4Ga$: C, 63.40; H, 5.67; N, 7.39. Found: C, 63.27; H, 5.73; N, 7.46. Analysis for Ga[(sal)$_3$tame-O-*sec*-Bu] (m.p. > 300°C) calculated for $C_{30}H_{32}N_3O_4Ga$: C, 63.40; H, 5.67; N, 7.39. Found: C, 62.94; H, 5.63; N, 7.37. Analysis for Ga[(5-MeOsal)$_3$tame-O-*n*-Pr] (m.p. > 300°C). Calculated for $C_{32}H_{36}N_3O_7Ga$: C, 59.64; H, 5.63; N, 6.52. Found: C, 59.67; H, 5.64; N, 6.46. Available quantities of Ga[(sal)$_3$tame-O-*iso*-Bu] (m.p. > 300°C) were insufficient for combustion analysis.

The molecular structure of Ga[(sal)$_3$tame-O-*iso*-Bu] was confirmed by x-ray crystallography using a single 0.20 × 0.20 × 0.05 mm colorless plate obtained from the ethanol reaction solution.

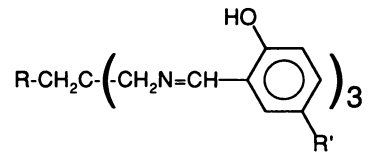

Ligand	R	R'	log *P*
H$_3$[(sal)$_3$tame-O-*n*-Bu]	-OCH$_2$CH$_2$CH$_2$CH$_3$	-H	3.10 ± 0.04
H$_3$[(sal)$_3$tame-O-*iso*-Bu]	-OCH$_2$CH(CH$_3$)$_2$	-H	3.10 ± 0.03
H$_3$[(sal)$_3$tame-O-*sec*-Bu]	-OCH(CH$_3$)CH$_2$CH$_3$	-H	2.58 ± 0.04
H$_3$[(5-MeOsal)$_3$tame-O-*n*-Pr]	-OCH$_2$CH$_2$CH$_3$	-OCH$_3$	2.54 ± 0.04

FIGURE 1. Structural formula of the *tris*(salicylaldimine) ligands studied and octanol/water partition coefficients, *P*, measured for the corresponding ^{67}Ga-complexes.

Data collection was performed with CuK$_\alpha$ radiation (1.54184 Å) using an Enraf-Nonius CAD4 computer-controlled kappa axis diffractometer equipped with a graphite crystal, incident beam monochromater. Monoclinic cell parameters for $C_{30}H_{32}GaN_3O_4$ at 293 ± 1 K: a = 11.8502(5), b = 12.716(1), c = 18.473(1) Å; β = 95.5(2)°; V = 2770(2)Å^3; Z = 4 in space group $P2_1/c$; $R(F_o)$ = 0.035, $R_w(F_o)$ = 0.047 for 3067 observed [I > 3.0 σ (I)] and absorption-corrected reflections. Hydrogen atoms were located and added to the structure factor calculations, but their positions were not refined.

The ^{67}Ga and ^{68}Ga complexes of the *tris*(salicylaldimine) ligands were prepared as described previously (*3,4*). Briefly, the HCl solution of the appropriate radionuclide was evaporated to dryness in a test tube while heating under a flow of N_2. The radioactive Ga^{3+} ion was redissolved in 50–100 μl ethanol containing 0.002 wt% acetylacetone and then 1–2 mg of the salicylaldimine ligand was added as an ethanol solution. This mixture was heated in a 70°C water bath for at least 10 min to form the gallium(III) *tris*(salicylaldimine) complex. The radiochemical purity of the products was evaluated by thin-layer chromatography on silica gel eluted with ethanol. All products were filtered through a sterile 0.2 μm polytetrafluoroethylene membrane (Millipore Corp., Bedford, MA) prior to use.

For rat biodistribution studies, the ^{67}Ga-complexes were diluted and injected as saline solutions containing 5% ethanol and 10%–15% propylene glycol. The biodistribution studies were conducted in male Sprague-Dawley rats following femoral vein injection of ca. 1–3 μCi of the ^{67}Ga complex in a volume of 0.1–0.2 ml, using previously described techniques (*12*). The reported heart-to-blood, heart-to-lung, and heart-to-liver ratios are based on the percentages of the injected dose per gram of wet tissue at the respective time points. The octanol/water partition coefficient, *P*, of each ^{67}Ga-tracer was also measured as described previously (*12*). The log *P* values reported in Figure 1 represent the mean (± standard deviation) of three measurements.

PET images of a normal mongrel dog were obtained with the SP-3000E camera (*14*) at Washington University. After a transmission scan for attenuation correction, a myocardial perfusion image was obtained with ^{15}O-water (using ^{15}O-carbon monoxide for blood-pool correction) following a standard protocol (*15,16*). After decay of the ^{15}O-tracers, 10 mCi ^{68}Ga[(sal)$_3$tame-O-*iso*-Bu] were administered intravenously in 4 ml saline containing 5% ethanol and 10% propylene glycol. TLC showed the ^{68}Ga radiopharmaceutical to have a radiochemical purity exceeding 98%. PET data were collected in list-mode for 45 min, commencing at the time of ^{68}Ga-injection. Myocardial time-activity curves were generated for ^{68}Ga[(sal)$_3$tame-O-*iso*-Bu] using selected regions of interest from consecutive images reconstructed in 3-min frames from the list-mode data.

RESULTS AND DISCUSSION

The synthesis of the ^{67}Ga complexes of the four *tris*(salicylaldimine) ligands (Fig. 1) proceeded smoothly following the method previously described (*3,4*). These complexes each migrated as single radioactive peaks near the solvent front (R_f = 0.85–0.89) on silica gel TLC plates eluted with ethanol, while their ^{67}Ga(acac)$_3$ precursor was found to remain at the origin. In all cases, the radiochemical purity of the products was found to exceed 98% (Fig.

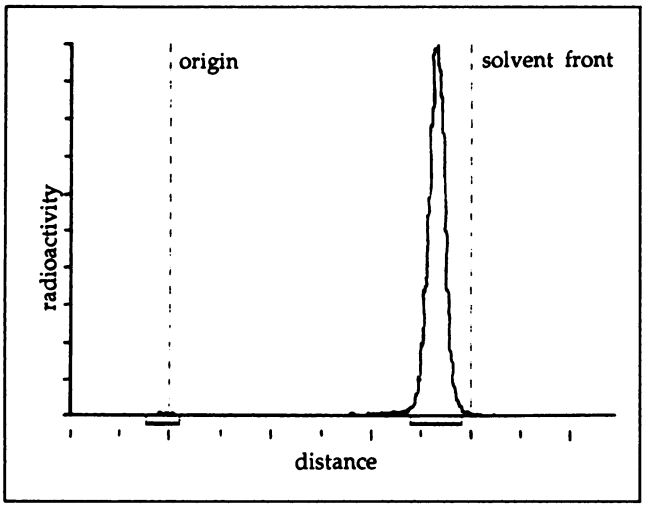

FIGURE 2. Typical thin-layer radiochromatogram demonstrates the radiochemical purity of the ^{67}Ga and ^{68}Ga complexes investigated. The radiochromatogram shown is for ^{67}Ga[(sal)$_3$tame-O-*iso*-Bu].

2). As expected, octanol/water partition coefficient measurements show these tracers to be quite lipophilic, with *log P* values ranging from 2.5 to 3.1 (Fig. 1). The x-ray crystal structure of Ga[(sal)$_3$tame-O-*iso*-Bu] (Fig. 3) confirms that this ligand affords a pseudo-octahedral $N_3O_3^{3-}$ coordination sphere for the Ga^{3+} ion as previously observed for the ring-substituted Ga[(5-MeOsal)$_3$tame] complex (*3,12*).

No particular effort was made to optimize the radiochemical yield of ^{68}Ga[(sal)$_3$tame-O-*iso*-Bu], since adequate quantities of product were readily available for the experiments of interest. Following the procedure described, the final saline/propylene glycol solution of Ga[(sal)$_3$tame-O-*iso*-Bu] was obtained with a decay-corrected radiochemical yield of 30%. Of the radioactivity that was lost, 27% was not re-solubilized from the test tube used for evaporation of the $^{68}Ga^{3+}$/1N HCl generator eluate, while 42% remained associated with the 0.2 μm PTFE membrane used for final filtration of the product. Additional pure product was recovered by washing the PTFE filter with ethanol but was not used. To insure aqueous solubility of these highly lipophilic Ga radiotracers, propylene glycol (10%–15%) was included in the preparations used for animal studies. Propylene glycol is a widely used pharmaceutical excipient with extremely low toxicity (*17*) and is expected to exert no pharmacological influence on myocardial perfusion in the animal studies conducted.

Following intravenous injection into rats, these ^{67}Ga complexes are all rapidly cleared from the blood and exhibit significant myocardial uptake (Tables 1–4). At 1 min post-injection, 2.4%, 2.0%, 2.1% and 1.1% of the injected dose was found in the heart for the ^{67}Ga[(sal)$_3$tame-O-*iso*-Bu], ^{67}Ga[(sal)$_3$tame-O-*n*-Bu], ^{67}Ga[(sal)$_3$tame-O-*sec*-Bu] and ^{67}Ga[(5-MeOsal)$_3$tame-O-*n*-Pr] complexes, respectively. The corresponding heart-to-blood ratios are quite high: 17 ± 3; 14 ± 2, 12 ± 2 and 3.5 ± 0.4 at 1 min and 14 ± 4, 10 ± 1, 10 ± 1 and 3.2 ± 0.1 at 5 min.

As would be expected for such lipophilic tracers, a large fraction of the injected radioactivity is taken up by the liver. Unfortunately, ^{67}Ga radioactivity was observed to progressively accumulate in the liver over the 1-hr time course of the rat biodistribution studies with the (sal$_3$tame-O-*iso*-Bu), (sal$_3$tame-O-*n*-Bu), and (sal$_3$tame-O-*sec*-Bu) complexes (Tables 1–3). The resulting high concentrations of ^{67}Ga in the liver could interfere with clearly visualizing the apex of the heart with PET. These three tracers contrast with the behavior of the [(5-MeOsal)$_3$tame-O-*n*-Pr] derivative, which is excreted from the liver into the bile (Table 4). A similar trend has been previously observed with gallium complexes of this type; Ga[(sal)$_3$tame] derivatives with alkoxy-substituents on the aromatic rings are consistently cleared from the liver into the bile, while liver

FIGURE 3. Stereoscopic ORTEP drawing showing the solid state molecular structure of Ga[(sal)$_3$tame-O-*iso*-Bu]. Selected bond distances (Å): Ga-O(12) 1.919[2]; Ga-O(22) 1.922[2]; Ga-O(32) 1.908[2]; Ga-N(11) 2.087[3]; Ga-N(21) 2.069[3]; Ga-N(31) 2.083[3]. Selected bond angles (degrees): O(12)-Ga-O(22) 93.32[9]; O(12)-Ga-O-(32) 92.62[9]; O(12)-Ga-N(11) 88.18[9]; O(12)-Ga-N(21) 93.6[1]; O(12)-Ga-N(31) 171.95[9]; O(22)-Ga-O(32) 92.08[9]; O(22)-Ga-N(11) 171.14[9]; O(22)-Ga-N(21) 87.0[1]; O(22)-Ga-N(31) 94.58[9]; O(32)-Ga-N(11) 96.57[9]; O(32)-Ga-N(21) 173.75[9]; O(32)-Ga-N(31) 88.64[9]; N(11)-Ga-N(21) 84.2[1]; N(11)-Ga-N(31) 83.8[1]; N(21)-Ga-N(31) 85.3[1]. (Numbers in brackets following bond distances and angles are the estimated standard deviations in the least significant digits.)

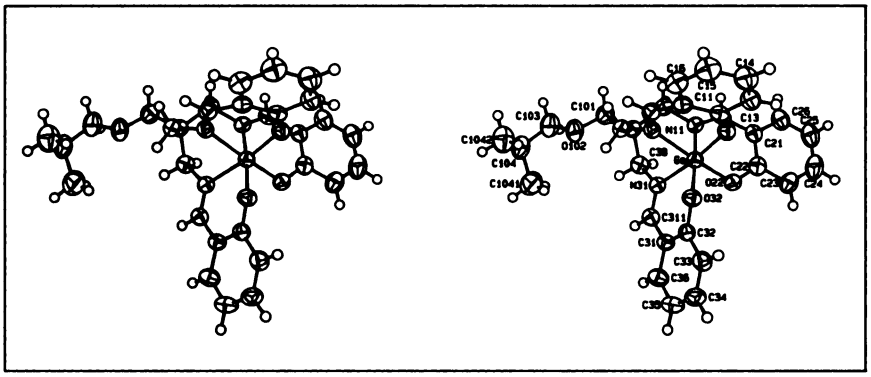

TABLE 1
Biodistribution of ^{67}Ga[(sal)$_3$tame-O-*iso*-Bu] in Rats*

Organ	% ID/Organ		
	1 min	5 min	60 min
Blood†	2.68 ± 0.56	1.50 ± 0.29	0.31 ± 0.05
Heart	2.39 ± 0.13	1.03 ± 0.02	0.15 ± 0.02
Lungs	2.11 ± 0.97	0.57 ± 0.11	0.15 ± 0.01
Liver	17.4 ± 1.3	26.7 ± 6.40	59.7 ± 3.9
Spleen	0.38 ± 0.08	0.29 ± 0.06	0.058 ± 0.009
Kidney (1)	3.78 ± 0.43	2.00 ± 0.07	0.29 ± 0.03
Brain	0.028 ± 0.002	0.021 ± 0.003	0.010 ± 0.002
Heart-to-Blood‡	*17.1 ± 2.8*	*14.3 ± 3.4*	*9.5 ± 0.7*
Heart-to-Lung‡	*2.7 ± 1.6*	*3.2 ± 6.2*	*1.8 ± 0.2*
Heart-to-Liver‡	*1.49 ± 0.05*	*0.42 ± 0.07*	*0.027 ± 0.004*

* Following bolus intravenous injection; values at each time point represent the mean of four rats, 176–199 grams.
† Blood was assumed to account for 7% of total body mass.
‡ Ratios calculated from the percentage of the injected dose per gram of tissue.

TABLE 3
Biodistribution of ^{67}Ga[(sal)$_3$tame-O-*sec*-Bu] in Rats*

Organ	% ID/Organ		
	1 min	5 min	60 min
Blood†	3.31 ± 0.23	1.62 ± 0.17	0.27 ± 0.06
Heart	2.07 ± 0.11	0.77 ± 0.09	0.11 ± 0.02
Lungs	1.08 ± 0.32	0.44 ± 0.08	0.116 ± 0.008
Liver	19.6 ± 3.6	25.2 ± 0.9	55.0 ± 3.7
Spleen	0.37 ± 0.07	0.21 ± 0.02	0.047 ± 0.005
Kidney (1)	3.49 ± 0.38	1.82 ± 0.26	0.24 ± 0.04
Brain	0.028 ± 0.002	0.015 ± 0.0008	0.011 ± 0.002
Heart-to-Blood‡	*11.8 ± 1.4*	*9.6 ± 1.4*	*7.9 ± 0.7*
Heart-to-Lung‡	*4.1 ± 1.3*	*3.7 ± 0.5*	*1.9 ± 0.4*
Heart-to-Liver‡	*1.3 ± 0.2*	*0.38 ± 0.06*	*0.025 ± 0.005*

* Following bolus intravenous injection; values at each time point represent the mean of four rats, 182–198 g.
† Blood was assumed to account for 7% of total body mass.
‡ Ratios calculated from the percentage of the injected dose per gram of tissue.

radioactivity accumulates and persists when the aromatic rings contain no functional substitutents at the 4, 5, or 6 positions (*3,4*). Despite being uncharged and lipophilic, none of these gallium-tracers were found to penetrate the blood-brain barrier.

The myocardial uptake of these new gallium *tris*(salicylaldimine) complexes in rats at 1 min postinjection significantly exceeds (>2×) that reported for ^{68}Ga[(5-MeOsal)$_3$tame] (*3*), strongly suggesting the new tracers are extracted from blood into myocardium more efficiently than ^{68}Ga[(5-MeOsal)$_3$tame]. Based on the rat biodistribution data for these complexes, Ga[(sal)$_3$tame-O-*iso*-Bu] was selected for further investigation in a PET imaging experiment. Excellent images of the dog heart were obtained from PET data collected from 2 to 10 min after intravenous injection of ^{68}Ga[(sal)$_3$tame-O-*iso*-Bu] (Fig. 4). As observed in the rat, lung and blood-pool radioactivity were both low during the 45-min time frame of image acquisition. These ^{68}Ga[(sal)$_3$tame-O-*iso*-Bu] myocardial images are much superior to those previously obtained with ^{68}Ga[(5-MeOsal)$_3$tame] (*3*), since the high heart-to-blood ratios afforded by the O-*iso*-Bu derivative obviate the need for blood-pool correction. However, just as in the rat, the ^{68}Ga[(sal)$_3$tame-O-*iso*-Bu] tracer was found to clear from dog myocardium rather rapidly (Fig. 5), with ^{68}Ga radioactivity accumulating in the liver.

Although good definition of the heart was obtained in PET images with ^{68}Ga[(sal)$_3$tame-O-*iso*-Bu], the observed rapid clearance of radioactivity from the myocardium may be undesirable. The clearance of ^{68}Ga-radioactivity from

TABLE 2
Biodistribution of ^{67}Ga[(sal)$_3$tame-O-*n*-Bu] in Rats*

Organ	% ID/Organ		
	1 min	5 min	60 min
Blood†	2.79 ± 0.51	1.47 ± 0.22	0.26 ± 0.03
Heart	2.01 ± 0.14	0.76 ± 0.11	0.09 ± 0.01
Lungs	1.07 ± 0.31	0.42 ± 0.08	0.11 ± 0.02
Liver	16.8 ± 4.3	25.4 ± 2.9	56.5 ± 2.2
Spleen	0.41 ± 0.04	0.23 ± 0.04	0.044 ± 0.009
Kidney (1)	2.74 ± 0.20	1.39 ± 0.14	0.17 ± 0.02
Brain	0.021 ± 0.004	0.016 ± 0.001	0.007 ± 0.001
Heart-to-Blood‡	*13.9 ± 1.7*	*9.6 ± 1.0*	*6.4 ± 0.3*
Heart-to-Lung‡	*4.2 ± 0.6*	*3.3 ± 0.6*	*1.4 ± 0.3*
Heart-to-Liver‡	*1.4 ± 0.6*	*0.36 ± 0.12*	*0.017 ± 0.002*

* Following bolus intravenous injection; values at each time point represent the mean of four rats, 173–194 g.
† Blood was assumed to account for 7% of total body mass.
‡ Ratios calculated from the percentage of the injected dose per gram of tissue.

TABLE 4
Biodistribution of ^{67}Ga[(5-MeOsal)$_3$tame-O-*n*-Pr] in Rats*

Organ	% ID/Organ		
	1 min	5 min	60 min
Blood†	6.23 ± 1.08	4.03 ± 0.29	1.51 ± 0.09
Heart	1.13 ± 0.09	0.70 ± 0.05	0.22 ± 0.03
Lungs	1.64 ± 0.26	0.71 ± 0.18	0.34 ± 0.03
Liver	26.6 ± 4.0	23.7 ± 2.6	9.36 ± 0.80
Spleen	0.48 ± 0.08	0.32 ± 0.07	0.14 ± 0.01
Kidney (1)	2.65 ± 0.35	1.35 ± 0.15	0.37 ± 0.04
Brain	0.034 ± 0.006	0.020 ± 0.002	0.015 ± 0.002
Heart-to-Blood‡	*3.4 ± 0.4*	*3.2 ± 0.1*	*2.4 ± 0.3*
Heart-to-Lung‡	*1.2 ± 0.2*	*1.5 ± 0.1*	*0.98 ± 0.19*
Heart-to-Liver‡	*0.44 ± 0.07*	*0.32 ± 0.04*	*0.21 ± 0.04*

* Following bolus intravenous injection; values at each time point represent the mean of four rats, 173–201 g.
† Blood was assumed to account for 7% of total body mass.
‡ Ratios calculated from the percentage of the injected dose per gram of tissue.

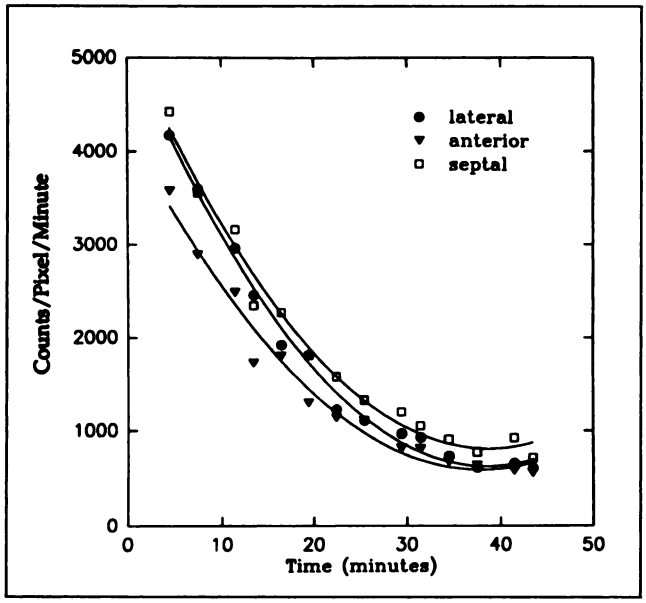

FIGURE 4. PET images of two adjacent 14.2 mm cross-sectional slices through the dog chest. All images are oriented with the animal's right to the reader's left and its spine at the bottom. Top: Myocardial perfusion images obtained with ^{15}O-water after subtraction of myocardial blood pool activity (determined with ^{15}O-carbon monoxide). Bottom: ^{68}Ga[(sal)$_3$tame-O-*iso*-Bu] images reconstructed using data acquired from 2–10 min postinjection. Note the excellent definition of the heart in the ^{68}Ga images *without* blood pool subtraction.

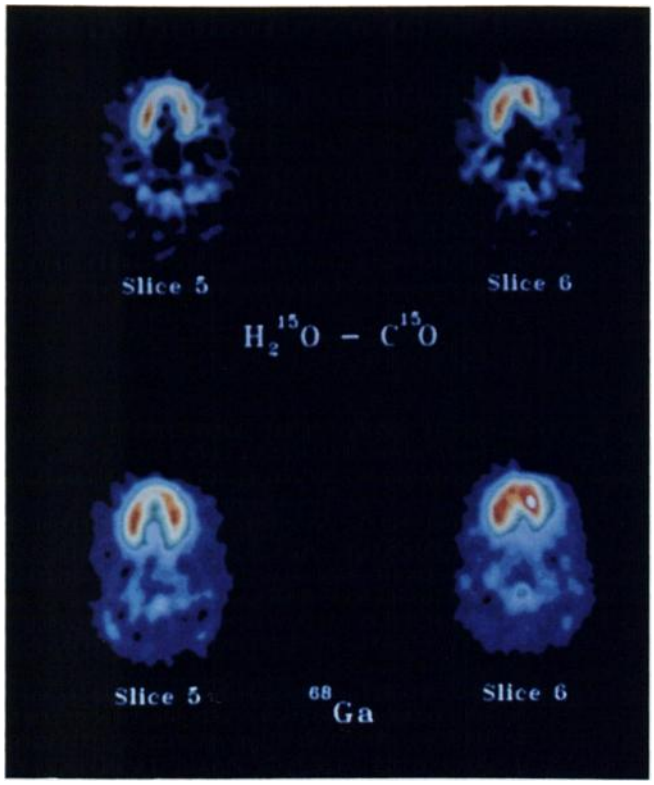

FIGURE 5. Time-activity curves for three myocardial regions using the data obtained in the PET study that produced the images shown in Figure 4.

myocardium could facilitate a second tracer injection for repeat imaging, somewhat analogous to the use of the ^{99m}Tc radiopharmaceutical, Cardiotec® (*18,19*). However, since the rate of tracer clearance from myocardium is likely to increase with the rate of perfusion, the contrast between high and low flow myocardial regions can be expected to progressively degrade with time following injection. Consequently, we believe it would be better to have a ^{68}Ga radiopharmaceutical that is retained in the heart, so that the 68-min half-life can be exploited with either long image acquisition periods and/or delayed imaging following administration. In addition, the liver accumulation and retention of ^{68}Ga radioactivity seen with this particular salicylaldimine complex would be prohibitive in clinical use due to the consequent radiation dose to the liver.

CONCLUSIONS

These new gallium *tris*(salicylaldimine) complexes are clearly superior to previous derivatives investigated as myocardial imaging agents with ^{68}Ga and PET. The ^{68}Ga-[(sal)$_3$ tame-O-*iso*-Bu] complex was found to provide excellent PET images of the dog heart; however, the pharmacokinetics of this tracer remain less than ideal. Further studies are in progress to evaluate related tracers that might provide the high heart uptake and heart-to-blood ratios seen with this tracer, while avoiding the problems associated with accumulation of ^{68}Ga radioactivity in the liver.

ACKNOWLEDGMENTS

Support for this research was provided by a grant from the National Cancer Institute (R01-CA46909). Gallium-68 for the PET experiment was provided by DOE grant DE-FG02-87ER60512. The authors wish to thank Steven R. Bergmann, MD, PhD, Carla J. Weinheimer, and Michael J. Welch, PhD at Washington University for performing the canine PET study.

REFERENCES

1. Green MA. The potential for generator-based PET perfusion tracers. *J Nucl Med* 1990;31:1641–1645.
2. Green MA, Welch MJ. Gallium radiopharmaceutical chemistry. *Nucl Med Biol* 1989;16:435–448.
3. Green MA, Welch MJ, Mathias CJ, Fox KAA, Knabb RM, Huffman JC. Gallium-68, 1,1,1-*tris*-(5-methoxysalicylaldiminomethyl)ethane: a potential tracer for evaluation of regional myocardial blood flow. *J Nucl Med* 1985;26:170–180.
4. Green MA. Synthesis and biodistribution of a series of lipophilic galliium-67 *tris*(salicylaldimine) complexes. *J Labelled Compd Radiopharm* 1986; 23:1227–1229.
5. Madsen SL, Welch MJ, Weisman RA, Motekaitis RJ, Martell AE. Synthesis and investigation of N,N,N′,N′-*tetrakis*(2-hydroxy-3,5-dimethylbenzyl)-ethylenediamine: a potential generator-produced tracer for PET imaging [Abstract]. *J Nucl Med* 1990;31:768.
6. Min M, Yutai J, Boli L, Lin Z. Studies on derivatives of BAT chelates labelled with ^{67}Ga, ^{113m}In, and ^{201}Tl. I. Labelling reactions of BAT derivative chelates and biodistribution in mice. *J Isotopes* 1989;2:36–40.
7. Kung HF, Liu BL, Mankoff D, et al. A new myocardial imaging agent: synthesis, characterization, and biodistribution of [^{68}Ga]BAT-TECH. *J*

Nucl Med 1990;31:1635–1641.
8. Harris WR, Pecoraro VL. Thermodynamic binding constants for gallium transferrin. *Biochemistry* 1983;22:292–299.
9. Neumann WL, Woulfe SR, Rogic MM, Dunn TJ. Synthesis of functionalized tripodal hexadentate ligand systems for Tc-99m radiopharmaceutical applications [Abstract]. *J Nucl Med* 1990;31:897.
10. Dunn TJ, Neumann WL, Rogic MM, Woulfe SR. Versatile methods of synthesis of differentially functionalized pentaerythritol amine derivatives. *J Org Chem* 1990;55:6368–6373.
11. Loc'h C, Maziere B, Comar D. A new generator for ionic gallium-68. *J Nucl Med* 1980;21:171–173.
12. Green MA, Welch MJ, Huffman JC. Synthesis and crystallographic characterization of a gallium salicylaldimine complex of radiopharmaceutical interest. *J Am Chem Soc* 1984;106:3689–3691.
13. John EK, Green MA. Structure-activity relationships for metal-labeled blood flow tracers: comparison of keto aldehyde *bis*-(thiosemicarbazonato)-copper(II) derivatives. *J Med Chem* 1990;33:1764–1770.
14. Bergmann SR, Ficke DC, Beecher D, Hood JT, Ter-Pogossian MM. Design parameters and initial testing of Super PET 3000-E: a whole body PET designed for dynamic cardiac imaging [Abstract]. *J Nucl Med* 1991;32:1838.
15. Bergmann SR, Fox KAA, Rand AL, et al. Quantification of regional myocardial blood flow *in vivo* with $H_2{}^{15}O$. *Circulation* 1984;70:724–733.
16. Bergmann SR, Herrero P, Markham J, Weinheimer CJ, Walsh MN. Noninvasive quantitation of myocardial blood flow in human subjects with oxygen-15-labeled water and positron emission tomography. *J Am Coll Cardiol* 1989;14:639–652.
17. Ruddick JA. Toxicology, metabolism, and biochemistry of 1,2-propanediol. *Toxicol Appl Pharmacol* 1972;21:102–111.
18. McSherry BA. Technetium-99m-teboroxime: a new agent for myocardial perfusion imaging. *J Nucl Med Techal* 1991;19:22–26.
19. Li QS, Solot G, Frank TL, Wagner HN, Becker LC. Tomographic myocardial perfusion imaging with technetium-99m-teboroxime at rest and after dipyridamole. *J Nucl Med* 1991;32:1968–1976.

(continued from page 198)

SELF-STUDY TEST
Pulmonary Nuclear Medicine

QUESTIONS *(continued)*

C. Reduced alveolar compliance, markedly reduced clearance time of ^{99m}Tc DTPA aerosol.
D. Decreased alveolar compliance, increased airways resistance, normal xenon clearance time.
E. Normal compliance, increased small airways resistance, normal or mildly heterogeneous regional xenon clearance time.

11. 28-year-old man with a 10 pack-year smoking history
12. 45-year-old woman with a 60 pack-year smoking history
13. 25-year-old man with a tibial fracture 1 week ago and acute onset of dyspnea
14. 25-year-old man with massive internal injuries resulting from a motor vehicle accident
15. 40-year-old woman with idiopathic pulmonary fibrosis

For each pattern of thoracic Ga uptake (items 16-20), select the most closely associated diagnosis (answers A-E)

A. sarcoidosis
B. *Pneumocystis carinii* pneumonia
C. primary lung cancer
D. chronic interstitial pneumonitis
E. bacterial pneumonia

16. Several small mediastinal foci and a larger, less well defined region of uptake in the right middle lobe.
17. Intense uptake limited to the right middle lobe.
18. Prominent uptake in both hilar regions and the right paramediastinal region, and diffuse bilateral lower lobe uptake.
19. Diffuse, bilateral high-intensity pulmonary uptake.
20. Irregular parenchymal uptake predominantly in the lower lung zones.

SELF-STUDY TEST
Pulmonary Nuclear Medicine

ANSWERS

Items 1-5: Ventilation-Perfusion Scintigraphic Patterns
Answers: 1, C; 2, C; 3, D; 4, E; 5, C

Ventilation-perfusion "matches" with a normal radiograph should be interpreted as indicating an intermediate probability for pulmonary embolism if the ventilation abnormalities involve more than 50% of the lung fields. When obstructive pulmonary disease is diffuse or extensive, it may not be possible to recognize coexisting ventilation-perfusion mismatching due to superimposed pulmonary embolism.

A single, unmatched perfusion defect, even if segmental in size, should be interpreted as an intermediate-probability finding. Some earlier interpretation schemes suggested that this finding indicated a high probability of pulmonary embolism; more recent studies, however, show that this scintigraphic pattern is associated with an intermediate probability.

When a perfusion defect is much larger than the associated radiographic opacity, the defect can be considered essentially as unmatched by the radiographic abnormality (assuming there is no ventilation abnormality in that part of the perfusion defect outside of the region of radiographic opacity). Thus, the finding of two segmental (large) perfusion defects with normal ventilation and only a small radiographic density associated with one of them, indicates a high probability of pulmonary embolism.

The chest radiograph should be obtained at approximately the same time as the scintigraphic study. In patients with stable clinical and radiographic findings, this interval could be as long as 18-24 hours. When the patient's clinical condition is changing or there are newly evolved radiographic abnormalities on prior films, the chest radiograph for comparison with the scintigrams should be obtained much closer in time to the ventilationperfusion study. In the situation described in Item 4 the infiltrate could have enlarged during the 18-hour interval to more closely match the perfusion abnormality in the superior segment. Additionally, new infiltrate may have developed in the posterior basal segment. The subtle washin abnormalities noted on the ventilation study suggest that

(continued on page 287)